Clutter-based metrics for radar-based breast imaging: clutter region selection

Stacey Torres
Trinity College Dublin,
College Green,
Dublin, Ireland
torress@tcd.ie

Declan O'Loughlin
Trinity College Dublin,
College Green,
Dublin, Ireland
d.oloughlin@tcd.ie

2026 International Conference on Medical Microwave Imaging Applications (ICMWIA) | 979-8-3315-6966-2/26/$31.00 ©2026 IEEE | DOI: 10.1109/ICMWIA67461.2026.11448370

***Abstract*—Results from first-in-human and later trials of microwave breast imaging continue to be reported with a variety of quantitative and qualitative findings in the literature. Clutter-based metrics are very widely reported, however, small differences in the implementations and definitions are common and restrict the ability to compare these values across findings. Using idealised images and experimental validation, two common versions of the signal-to-mean ratio (SMR) are compared and the maximum and typical differences in the final values examined. For the largest signal regions, difference of up to $10\,\%$ could be expected, with the largest differences observed in homogeneous breast phantoms. Based on these findings, not including the signal region in the clutter region for SMR is recommended to match the only practical definition of the signal-to-clutter ratio (SCR).**

***Index Terms*—component, formatting, style, styling, insert**

I. Introduction

Microwave breast imaging has seen increasing use in early-stage clinical trials, with both research and commercial prototypes in development and use. Recent human results include a second in-human trial of 62 participants with the Wavelia system [1], further results from the commercial MARIA system with 389 participants in [2], breast density estimates with 110 participants using the TSAR system [3]. Protocols for up to 10 000 participants have also been published for the MammoWave system in [4]. Due to the increasing volume of human data reported in the literature, now in the thousands of people, comparisons and systematic reviews of the findings and results are increasingly common, including work on how the image quality and efficacy of microwave breast images can be measured, how clinical efficacy can be shown and tools and techniques for measuring and reporting quality [5]–[8]. For radar-based images, one category of clutter-based metric has been very widely reported, commonly called signal-to-mean ratio (SMR).

Although the SMR and related contrast-based metrics are widely reported, it is difficult to compare across studies as the terms are loosely defined [6]. Similarly, the contrast-based metrics can be of limited value for certain comparisons as many functions when applied to the image can increase the contrast as measured this way without adding new information. Any function which increases the energy in the signal region by more than clutter region such as squaring will always increase the SMR. However, when used as part of a series of comparisons or when used to quantify a qualitative assessment of an image, the SMR can still be useful. Furthermore, due the volume of these metrics reported, they are a useful quantitative comparator where the implementations are understood.

This work was supported by the Trinity College Dublin Boost Programme.

As described in [5], [6], contrast-based metrics are typically calculated by selecting a signal and a clutter region and calculating a summary statistic over the points in those regions. The most common implementation of SMR uses the maximum value of both signal region and the mean value of the clutter region. A similar metric is the signal-to-clutter ratio (SCR) which uses the maximum in both regions, however, SCR can be sensitive to the amplitudes of individual points in the imaging domain which may or may not be relevant to the image interpretation. Typically in qualitative interpretations, such individual high amplitude points would not be considered as important. In some cases, the clutter region includes the signal region, in others, it does not.

In this work, the maximum possible differences between the SMR calculated with clutter regions that include or do not include the signal regions are calculated. Firstly, given representative sizes of signal regions, imaging resolutions and imaging domains, the worst-case difference is estimated assuming that the signal region has maximum intensity and the clutter region has minimum intensity. Secondly, the measured differences for images from the BRIGID database in [9] are calculated and compared to the maximum possible differences. In both cases, the signal region is centered on the point of maximum intensity in the image.

The remainder of this work is structured as follows: the description of the imaging domain and how the metrics are calculated is described in section II along with the experimental comparisons, the maximum differences and measured differences are discussed in section III and section IV concludes the paper.

II. Methods

A typical imaging domain is a hemispherical or cylindrical volume which is discretised into a set of points, $\mathbf{P}$. In this work, a representative hemispherical domain based on the MERIT prototype in [9] is used with radius of $7\,\mathrm{cm}$. The

979-8-3315-6966-2/26/$31.00 ©2026 IEEE

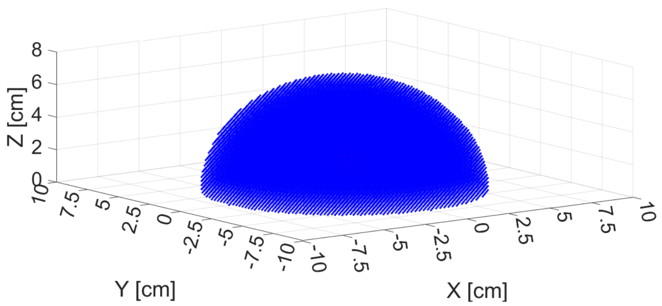

Fig. 1. A $7\,\mathrm{cm}$ radius hemisphere with a dense array of imaging points on a rectangular grid as is common for radar-based microwave breast images. In some prototypes, the imaging domain may be different from scan to scan depending on the breast size if the antennas are fixed and not in contact with the breast. In other systems, the antennas are in direct or near direct contact with the breast.

number of points in the imaging domain, $\#\mathbf{P}$, depends on the resolution, r. For contrast-based metrics, the imaging domain is segmented into a signal region, $\mathbf{S}$, such that $\mathbf{S} \subseteq \mathbf{P}$. The clutter region can then be defined either including or not including the signal region, such that $\mathbf{C}^T = \mathbf{P}$ or $\mathbf{C}^O = \mathbf{P} \setminus \mathbf{S}$.

A. Signal Region Selection

The set of points in the signal region, $\mathbf{S}$, can be selected in at least two ways depending on either:

- *a priori* knowledge of the tumour or target location without regard to the image;
- or the maximum response in the image without regard to known areas of interest.

Both cases have very different results, if the signal region, $\mathbf{S}$, is centered on the maximum response in the image, this means that the SMR is always greater than one, or positive when expressed in dB. Regions of interest are often not well known in clincal data or when reviewing images blinded to clinical status, and where such information is known, alternative metrics for estimating localisation exist. Therefore, the SMR is commonly measured based on characteristics of the image alone and interpreted along with separate localisation metrics.

The signal region itself can be an ellipsoidal, spherical, cuboidal or irregularly shaped region centered on the chosen point [5]. Due to the discretisation of the domain, there is little difference between these shapes for small regions for coarser resolutions. The size of the signal region is either based on *a priori* information, on characteristics of the image or a combination of both. For the signal-to-clutter ratio (SCR), the size of the region is particularly important, as if the boundary of the signal region does not extend far enough, the maximum value of the clutter region, just outside the boundary, may include points that are part of the main response of the image and not correctly quantify the response. However, the SMR is less sensitive to the precise radius of the signal region as the SMR compares the maximum intensity of the image to the mean energy in the rest of the image. In this study, the points in the signal region, $\mathbf{S}$, are in a uniform sphere of radius, R, centered at the point of maximum brightness in the image.

B. Clutter Region Determination

The SMR, Φ, is defined as:

$$\Phi = \frac{\max I[\mathbf{S}]}{\langle I[\mathbf{C}] \rangle} \tag{1}$$

or the maximum value of the image in the signal region divided by the mean of the image values in the clutter region. The mean intensity of the whole imaging domain, $\langle I[\mathbf{P}] \rangle$, is the weighted mean of the signal and clutter regions:

$$\langle I[\mathbf{P}] \rangle = \frac{\#\mathbf{C}}{\#\mathbf{P}} \langle I[\mathbf{C}] \rangle + \frac{\#\mathbf{S}}{\#\mathbf{P}} \langle I[\mathbf{S}] \rangle \tag{2}$$

where $\#\mathbf{P} = \#\mathbf{S} + \#\mathbf{C}$. If the size of the signal region is much smaller than the clutter region, $\#\mathbf{S} \ll \#\mathbf{C}$, then the difference in the mean of the clutter region by both definitions will be small, $\left\langle I[\mathbf{C}^T] \right\rangle \approx \left\langle I[\mathbf{C}^O] \right\rangle$. The largest difference will be when the mean of the signal region is the maximum intensity and the mean of the clutter region is of the lowest intensity. Normalising such that the maximum intensity is one, this means $\langle I[\mathbf{S}] \rangle = 1$ and $\langle I[\mathbf{C}] \rangle = 0$. Therefore, the difference between the means of the clutter area depending on whether the clutter area includes the signal area or not is:

$$\left\langle I[\mathbf{C}^T] \right\rangle - \left\langle I[\mathbf{C}^O] \right\rangle = \frac{\#\mathbf{S}}{\#\mathbf{P}} \tag{3}$$

For the hemispherical and spherical regions in this study, the number of points in a given region for a known resolution and radius, related to the Gauss Circle problem [10], can be approximated by dividing the volume of the imaging domain by the volume of a voxel. In the following results, the differences in SMR for resolutions of $0.5\,\mathrm{mm}$ to $5\,\mathrm{mm}$ are evaluated for signal regions between $10\,\mathrm{mm}$ to $30\,\mathrm{mm}$.

C. Experimental validation

To understand how the characteristics of experimental images correspond to the idealised images analysed in this work, the same metrics were calculated for the imaging from the BRIGID database [9]. Five different phantoms of increasing glandular content can each be imaged with twenty-two different tumour shapes as fully described in [11]. The same definitions of SMR are used, where the signal region is centered on the maximum response in the image. For the 110 images, the SMR with a clutter region including and not including the signal region is calculated. The averaged difference for each phantom is calculated and compared to the largest possible difference.

III. Results

The theoretical maximum differences between the mean of the whole image, $\left\langle I(C^T) \right\rangle$ and the mean of the clutter region excluding the signal region, $\left\langle I(C^O) \right\rangle$, is shown in fig. 2 along with the same calculations for 110 different images from the BRIGID dataset [9].

Firstly, the theoretical maximum differences are shown labelled from $r = 0.5\,\mathrm{mm}$ to $r = 5\,\mathrm{mm}$. The largest differences are seen for the finest resolutions, although, even for the largest signal regions of a $30\,\mathrm{mm}$ sphere in a $70\,\mathrm{mm}$ hemisphere,

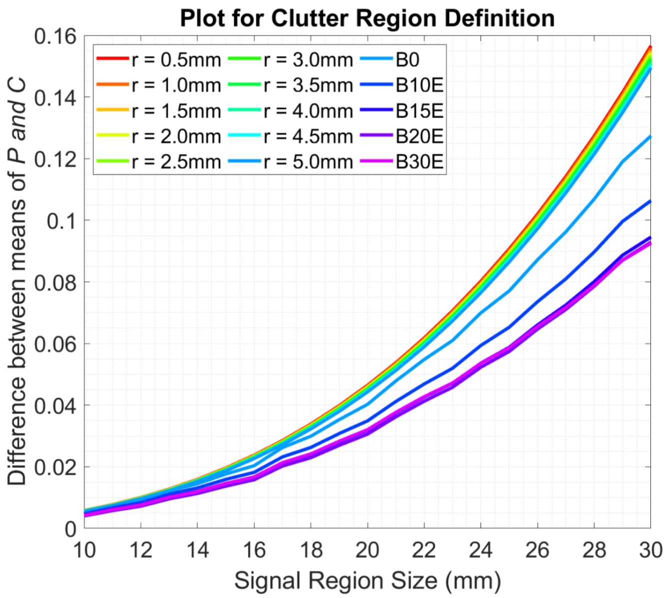

Fig. 2. The maximum differences between the mean of an clutter region and the mean of the whole image for a normalised, idealised image. Also shown are the average percentage differences for images of 22 different tumours in five different breast phantoms of increasing density (B0 to B30E).

there is less than a $1\,\%$ difference due to the resolution. The maximum difference increases as the resolution becomes finer, this is due to the spherical signal region compared to the hemispherical imaging domain, as the resolution becomes finer, there is a greater surface area in the signal region to gain voxels.

The experimental results are also shown in fig. 2. As can be seen, the difference between definitions is largest for the homogeneous breast phantoms. This is primarily because the images in homogeneous phantoms approximate the idealised images, where the amplitude in the signal region is much larger than the mean of the rest of the image. However, even in the most dense breast phantoms, there was up to a $10\,\%$ difference between the two definitions for the largest signal regions.

IV. Conclusions

Clutter-based metrics for microwave breast imaging have been extensively reported across various prototypes and can be useful for comparing images and performance. However, it is difficult to compare many of these metrics directly as they do not use the same definitions or methodology to calculate the values. One key difference is in the definition of clutter regions and whether they include or do not include the signal region.

This work suggests that the worst case differences between the SMR when calculated with the two different types of clutter region can be over $10\,\%$ for the largest signal regions in a hemispherical imaging domain. When compared to experimental images, the SMR measured in homogeneous breast phantoms showed the largest differences between values, but differences of up to $8\,\%$ can be seen in the most heterogeneous and dense breast phantoms. As the SCR, another commonly used clutter-based metric relies on not including the signal region in the clutter region, it is recommended to use a clutter region exclusive of the signal region in general.

Although widely reported, SMR and other clutter-based metrics have limitations. In particular, many trivial algorithms can artificially increase these metrics without adding new information, which means they cannot be used as a basis for comparison alone. However, SMR and the other clutter-based metrics may be a useful quantifier of how the image is interpreted and how prominent the main image peaks are.

References

[1] Fasoula, A.; Papatrechas, G.; Arvanitis, P.; Duchesne, L.; Gil Cano, J.D.; O'Donnell, J.; Abd Elwahab, S.; Kerin, M. Wavelia Microwave Breast Imaging Phase 2 Clinical Investigation: Methodological Evolutions and Multidimensional Radiomics Analysis Towards Controlled Specificity. Cancers 2025, 17, 2973. https://doi.org/10.3390/cancers17182973

[2] Richard Sidebottom, Donna Webb, Briony Bishop, Kabir Mohammed, Steven Allen, Results for the London investigation into dielectric scanning of lesions study of the MARIA® M6 breast imaging system, British Journal of Radiology, Volume 97, Issue 1155, March 2024, Pages 549–552, https://doi.org/10.1093/bjr/tqae013

[3] P. Mojabi, J. Bourqui, B. -J. Docktor, R. Y. Tsang and E. Fear, "Assessment of Breast Composition with A Transmission-based Microwave Imaging System," in IEEE Transactions on Biomedical Engineering, doi: 10.1109/TBME.2025.3584669

[4] Álvarez Sánchez-Bayuela D, Fernández Martín J, Tiberi G, et al. Microwave imaging for breast cancer screening: protocol for an open, multicentric, interventional, prospective, non-randomised clinical investigation to evaluate cancer detection capabilities of MammoWave system on an asymptomatic population across multiple European countries, BMJ Open 2024;14:e088431. doi: 10.1136/bmjopen-2024-088431

[5] E. Porter and D. O'Loughlin, "Pathway to Demonstrating Clinical Efficacy of Microwave Breast Imaging: Qualitative and Quantitative Performance Assessment," in IEEE Journal of Electromagnetics, RF and Microwaves in Medicine and Biology, vol. 6, no. 4, pp. 439-448, Dec. 2022, doi: 10.1109/JERM.2022.3218756

[6] Reimer, T.; Pistorius, S. Review and Analysis of Tumour Detection and Image Quality Analysis in Experimental Breast Microwave Sensing. Sensors 2023, 23, 5123. https://doi.org/10.3390/s23115123

[7] B. R. Lavoie, J. Bourqui, E. C. Fear and M. Okoniewski, "Metrics for Assessing the Similarity of Microwave Breast Imaging Scans of Healthy Volunteers," in IEEE Transactions on Medical Imaging, vol. 37, no. 8, pp. 1788-1798, Aug. 2018, doi: 10.1109/TMI.2018.2806878

[8] D. J. Kurrant, M. Omer and E. C. Fear, "Automated Workflow for Evaluating Microwave and Multi-Modality Breast Images," in IEEE Journal of Electromagnetics, RF and Microwaves in Medicine and Biology, vol. 7, no. 3, pp. 290-300, Sept. 2023, doi: 10.1109/JERM.2023.3289767

[9] D. O'Loughlin et al., "Sensitivity and Specificity Estimation Using Patient-Specific Microwave Imaging in Diverse Experimental Breast Phantoms," in IEEE Transactions on Medical Imaging, vol. 38, no. 1, pp. 303-311, Jan. 2019, doi: 10.1109/TMI.2018.2864150

[10] OEIS Foundation Inc. (2025), The On-Line Encyclopedia of Integer Sequences, Published electronically at https://oeis.org.

[11] Bárbara L Oliveira et al 2018 Biomed. Phys. Eng. Express 4 025036